



Open Archive Toulouse Archive Ouverte (OATAO)

OATAO is an open access repository that collects the work of Toulouse researchers and makes it freely available over the web where possible.

This is an author-deposited version published in: <http://oatao.univ-toulouse.fr/>
Eprints ID: 5842

To link to this article: DOI:10.1016/J.CEJ.2010.09.040
URL: <http://dx.doi.org/10.1016/J.CEJ.2010.09.040>

To cite this version: Jamnongwong, Marupatch and Loubiere, Karine and Dietrich, Nicolas and Hebrard, Gilles (2010) Experimental study of oxygen diffusion coefficients in clean water containing salt, glucose or surfactant: Consequences on the liquid-sidemass transfer coefficients. *Chemical Engineering Journal*, vol. 165 (n°3). pp. 758-768. ISSN 1385-8947

Any correspondence concerning this service should be sent to the repository administrator: staff-oatao@listes.diff.inp-toulouse.fr

Experimental study of oxygen diffusion coefficients in clean water containing salt, glucose or surfactant: Consequences on the liquid-side mass transfer coefficients

Marupatch Jamnongwong^{a,b,c}, Karine Loubiere^{d,e}, Nicolas Dietrich^{a,b,c}, Gilles Hébrard^{a,b,c,*}

^a Université de Toulouse, INSA, Laboratoire d'Ingénierie des Systèmes Biologiques et des Procédés (LISBP), 135 Avenue de Rangueil, 31077 Toulouse, France

^b INRA, UMRA792, LISBP, 31400 Toulouse, France

^c CNRS, UMR5504, LISBP, 31400 Toulouse, France

^d Université de Toulouse, INPT, UPS, Laboratoire de Génie Chimique, 4 Allée Emile Monso, F-31432 Toulouse, France

^e CNRS, Laboratoire de Génie Chimique, F-31432 Toulouse, France

A B S T R A C T

This present paper proposes new investigations aiming at: (i) studying the effect on oxygen diffusion coefficients of the presence in clean water of some compounds usually encountered in biological media and (ii) quantifying their consequences on liquid-side mass transfer coefficients. The oxygen diffusion coefficients D were firstly measured in various synthetic liquid phases containing either salt (NaCl), sugar (glucose) or surfactant (sodium laurylsulphate). When compared to clean water, noticeable reductions of D were observed; the variation of D with the compound concentration C was modelled and found dependent on the nature of the compound added. In a second time, using the same liquid media, experiments on a train of bubbles rising in a quiescent liquid phase were carried out to determine the associated liquid-side mass transfer coefficients (k_L). For all cases, as for diffusion coefficients, a decrease of k_L with increasing C was clearly observed whatever the aqueous solutions. These findings firstly showed that, even if the properties of clean water (density, viscosity, surface tension) were not significantly changed by the addition of salts (NaCl), the liquid-side mass transfer coefficients could be, all the same, modified. For the aqueous solutions of glucose, the reduction of k_L with diffusion coefficients D was well correlated, and mainly due to the change in viscosity with concentration. For surfactants, the hydrodynamic conditions (*i.e.* bubble Reynolds number) being almost kept constant for all concentrations, only the change in oxygen diffusion coefficients was thus responsible for the decrease of k_L . The present study clearly confirmed the need to complete and/or account for the database related to oxygen diffusion coefficients in complex media, this condition being imperatively required to describe and to model appropriately the gas-liquid mass transfer phenomena.

1. Introduction

The gas-liquid mass transfer, with the gas as dispersed phase, plays a key role in bioreactors (*i.e.* urban wastewater biological treatment, fermentation) as controlling the oxygen available for the microorganism metabolism. The performances of the biological process, as well as the associated energy consumption, are thus directly linked to the efficiency of the latter transfer phenomenon. Bioprocesses involve liquid media (culture broths) which are far more complex than a pure air-water system, as

containing many species (salts, hydrocarbons, alcohols, organic nutrients, surfactants. . .). The research devoted to gas-liquid mass transfer in bioprocess has been intensive for many years [1] but, paradoxically, the question is still approached in terms of volumetric mass transfer coefficients ($k_L a$). The physico-chemical properties of this complex environment and their impact on the mass transfer rates are thus considered together, namely by introducing the α -factor. This scaling factor is defined by [2]:

$$\alpha = \frac{(k_L a)_{\text{process water}}}{(k_L a)_{\text{clean water}}} \quad (1)$$

The α -factor remains widely used to account for process conditions when sizing aeration systems. The limit of such an approach is that the volumetric mass transfer coefficient is the global result of both contributions: the resistance to mass transport in the liquid side (k_L) and the interfacial area (a). The properties of the

* Corresponding author at: Université de Toulouse, INSA, Laboratoire d'Ingénierie des Systèmes Biologiques et des Procédés (LISBP), 135 Avenue de Rangueil, 31077 Toulouse, France. Tel.: +33 0 5 61 55 97 89; fax: +33 0 5 61 55 97 60.

E-mail address: Gilles.Hebrard@insa-toulouse.fr (G. Hébrard).

Nomenclature

a	interfacial area (L^{-1})
C	concentrations of salt/sugar/surfactant compound in clean water (ML^{-3})
C_L^*	dissolved oxygen concentration at saturation in the liquid phase (ML^{-3})
CMC	critical micelle concentration of the anionic surfactant (ML^{-3})
D	oxygen diffusion coefficient in the liquid phase under test ($L^2 T^{-1}$)
k_{La}	volumetric gas–liquid mass transfer coefficient (T^{-1})
k_L	liquid-side mass transfer coefficient (LT^{-1})
N	rotation speed of the magnetic agitator (T^{-1})
U_i^*	interfacial momentum transfer velocity (LT^{-1})
T	temperature (K)
H_L	height of liquid (L)
U_B	bubble velocity (L)
V_L	volume of liquid (L^3)
M	molar mass (L)
f	frequency (T^{-1})
m	mass (M)
d_B	bubble diameter (L)
Q	flow rate ($L^3 T^{-1}$)

Greek letters

μ	viscosity ($ML^{-1} T^{-1}$)
ρ	density (ML^{-3})
σ_L	tension force (MT^{-2})

Dimensionless number

Re_B	bubble Reynolds number $Re_B = ((\rho_L \cdot U_B \cdot d_B) / \mu_L)$
Sc	Schmidt number $Sc = (\mu_L / (\rho_L \cdot D))$
Sh	Sherwood t number $Sh = (k_L \cdot d_B / D)$

Abbreviation

CAS	chemical abstracts service
CMC	critical micelle concentration
std	mean standard deviation defined as $(1/N) \sum_{i=1, N} (X_{exp} - X_{theo}) / X_{exp}$

liquid phase may affect differently the mass transfer rates and the mechanisms of the physical processes involving bubbles (bubble formation, coalescence and break-up). So, due to its empirical nature, the α -factor does not enable the impact of the liquid medium properties on the performances of aeration neither to be fully understood nor to be predicted. This point was already highlighted by Zlokarnik [3] who studied the sorption characteristics of slot injectors and their dependency on the coalescence behaviour of the system (addition of salts and/or solids, such as cellulose, activated carbon). He clearly demonstrated that the coalescence behaviour of a system could not be described by means of a material-parameter alone, and that the enhancement factor (α) depended on the interaction of material and process-related parameters and on the type of the gas dispersing device. Hence, he concluded “there is no physical justification for the so-called “ α -factor” which is still widely used in waste-water treatment and is regarded as a material parameter”. Recently, Fyferling et al. [4] have compared, for concentrated microbial cultures (40–80 g of biomass dry mass per litre), the mass transfer coefficients obtained in biological media (culture broth or supernatant mineral media), and also in coalescing and non-coalescing mineral

media (composed of the main salts of the culture medium). These authors have observed that, even if the hold-up in the culture broth and in the corresponding supernatant matches the non-coalescing mineral medium, the k_{La} values calculated online (gas balance method) are, for a given dissipated power (ranged from 1 to 40 kW m⁻³), 4–8 times lower than the ones determined in the non-coalescing mineral medium. These findings have been explained using the three enhancement factors proposed by Sundararajan and Ju [5], relating to: (i) the changes of the chemical medium properties by the cell activity, (ii) the presence of solid particles, and (iii) the mass transfer enhancement by the reaction. However, no accurate quantification or modelling of each contribution was investigated.

More academic researches have been carried out on the impact of trace amounts of surfactants on bubble hydrodynamics (size, shape, rise velocity, drag coefficient) and on gas–liquid mass transfer. They have converged towards the idea that surface-active components induce two opposite effects: (i) on the one side, delaying the coalescence of gas bubbles and thus making the gas–liquid interfacial area larger, (ii) and on the other side, reducing the disturbance in the bulk fluid by resisting the interface motion, and thus making the resistance to mass transfer larger and liquid-side mass transfer coefficients smaller. Generally, these effects are taken into account [6–8]:

- by introducing the stagnant cap model (the adsorbed surfactants molecules are assumed to be dragged towards the rear of the bubble by adjacent liquid, a surface coverage ratio by active molecules is then defined),
- and/or by modifying the slip condition at the bubble surface (the surface of bubbles will be partially mobile or fully immobile depending on the concentration of active species),
- and/or by considering two liquid-side mass transfer coefficients (one for the clean front of the bubble, the other for the stagnant cap) whose contributions are weighted depending on the degree of coverage of the bubble surface.

Other authors [9,10] suggested that the action of surfactants would induce also an additional resistance in the liquid layers surrounding the bubbles, namely a change in diffusion coefficients. A gas transfer reduction of 30–70% of clean water values in surfactant solutions was observed by Rosso et al. [11]: according to them, by accumulating at the interface, surfactants lower the surface tension, reduce the interfacial renewal and the diffusion of gas into the liquid. Hébrard et al. [12] experimentally correlated, in clean water and in water contaminated by surfactants, the variations of liquid-side mass transfer coefficients k_L (for a train of bubbles) with changes of oxygen diffusion coefficients (an experimental device was developed to measure them). They pointed out an important issue, namely the need to determine the “true” diffusion coefficients of oxygen in multi-component solutions for an accurate modelling of the elementary mechanisms occurring in mass transfer phenomena; indeed, the oxygen diffusion coefficients encountered in the available literature are mainly defined for “clean” or mono-component liquid phase [13,14]. Very recently, Martin et al. [15] studied, from a theoretical point of view, the effect of surface tension and contaminants (salts) on mass transfer rates. The originality of this paper was to integrate the contribution of contaminants simultaneously into specific contact areas (using a population balance with proper theoretical closures for bubble coalescence efficiency, for partially and fully immobile surfaces, and bubble break-up), and liquid–film resistance (modelling as function of the coverage of the surface of the bubbles). They found that the degree of bubble surface coverage did not only affect bubble coalescence but also their break-up, that the ion strength defined bubble stability and critical Weber number, and that the

mass transfer rates were function of the surface coverage by the electrolytes.

In keeping with this scientific context and following the work of Hébrard et al. [12], the present paper proposes new experimental investigations, in which the effect of the presence in clean water of some compounds usually encountered in biological media (*i.e.* salt, sugar, surfactant) is analyzed. The true oxygen diffusion coefficients (namely the ones measured in the liquid media under test) will be firstly determined. Then, the impact of the active species on the liquid-side mass transfer coefficients associated with a train of calibrated bubbles will be determined, enabling thus some conclusions to be drawn.

2. Materials and methods

2.1. Gas and liquid phases

Compressed air and nitrogen from laboratory lines were the gas phases here used. Both particle-retention and activated-carbon filtering were used to avoid any unwanted contamination (such as solid particles or organic substances). Clean water was prepared by means of ion exchanger and activated-carbon filtering. Note that, at 20 °C, the conductivity of this *clean* water was almost 0.1–0.2 $\mu\text{S cm}^{-1}$ (WTW[®] Conductivity Meter LF538), the total organic carbon 0.2 ppm (Shimadzu[®] TOC-VCSH analyzer) and the pH 7.3 (WTW[®] Microprocessor pH Meter pH539).

To prepare synthetic liquid phases, the *clean* water previously described was used and combined with three types of compounds: a salt (NaCl), a sugar (glucose), or an anionic surfactant (sodium laurylsulphate). They were selected as commonly encountered in biological media. The surfactant here used (CAS 68891-38-3, Sidobre Sinnova[®]) was fully characterised in [9], in particular the critical micelle concentration (1.9 g L^{-1}) and various adsorption characteristics. Different concentrations of these compounds were tested:

- from 1.6 to 100 g L^{-1} for NaCl solutions (58 g mol^{-1} in molar mass),
- from 0.05 to 100 g L^{-1} for glucose solutions (180 g mol^{-1} in molar mass),
- from 0.05 to 1.9 g L^{-1} for surfactant solutions (382 g mol^{-1} in molar mass).

Note that, in addition to the precautions taken in the process steps for producing the gas phase and clean water, a great care was taken for the cleaning procedure of vessels between experiments. In particular, several rinse cycles were systematically carried out, the clean inside surfaces of vessel were not touched with fingerprint, and the clean reactor was close to the air (due to dust contamination).

For each solution, the density (ρ_L), the dynamic viscosity (μ_L) and the static surface tension (σ_L) were measured respectively by means of a pycnometer ($\rho_L \pm 0.2 \text{ kg m}^{-3}$), the viscometer RM180 Rheomat Rheometric Scientific[®] ($\mu_L \pm 10^{-3} \text{ mPa s}$) and the GBX[®] 3S tensiometer ($\sigma_L \pm 0.5 \text{ mN m}$). The latter physico-chemical properties are reported in Table 1 for each synthetic liquid phase. These measurements firstly show that salt and surfactant do not modify the viscosity whereas there is a noticeable rise in viscosity with the concentrations in glucose (until 1.26 mPa s at $C = 100 \text{ g L}^{-1}$). Concerning density, their variations with concentration never exceed 2% when compared to water; except for $C = 100 \text{ g L}^{-1}$, where they are slightly higher (+6.8% for salt and +3.8% for glucose).

Taking account for experimental uncertainties, the surface tensions of sugar solutions do not differ from the one of clean water ($\sigma_L = 72.8 \text{ mN m}^{-1}$), the most concentrated solution excepted ($\sigma_L = 65.4 \text{ mN m}^{-1}$). In salt solutions, they are slightly higher than in

clean water, reaching 76.1 mN m^{-1} for the highest concentration. This phenomenon often exists in presence of inorganic substances (salts of mineral acids, other electrolytes and ionic solutions), and is caused by the fact these molecules are repelled from the interface where they adsorb negatively [16]. On the contrary, the addition of surfactants to clean water strongly lowers the surface tensions ($\sigma_L = 39.7\text{--}69.8 \text{ mN m}^{-1}$ [12]). It is interesting to note that, for this surfactant, the characteristic time for reaching adsorption equilibrium at the gas–liquid interface is about 200 ms (as reported by [17]). It was significantly smaller than:

- the mean residence times (H_L/U_B) of the bubbles generated (see Section 2.3 and Table 4), which order of magnitude is 900 ms,
- the time characteristic for gas–liquid mass transfer ($1/k_L a$), which order of magnitude is above 60 min for the experiments in the double-wall vessel (Section 2.2) and varies between 300 and 600 s for the experiments involving the bubble' train (Section 2.3).

Hence, it can be reasonably assumed that the adsorption equilibrium of the surfactant molecules at the gas–liquid interface is reached in the experiments run (justifying thus to consider “static” surface tensions rather dynamic surface tension). For the same reason (*i.e.* the time-scale domain), the diffusion coefficients measured becomes time-independent parameters.

2.2. Experimental set-up for measuring oxygen diffusion coefficients (free-interface device)

As presented in [12], the determination of oxygen diffusion coefficients was based on measurements of volumetric mass transfer coefficients ($k_L a$) occurring at a free gas–liquid interface under controlled hydrodynamics conditions. For that, a specific experimental facility was designed (Fig. 1), consisting in a double-wall glass vessel, tightly closed, filled with a known height of liquid (0.035 m). Bulk agitation of liquid was ensured by a magnetic agitator rotating at a very small speed (100 rpm) so as to maintain a constant flat surface of the gas–liquid interface whatever the experiments. The temperature of the liquid phase was maintained at 20 °C. The experiments were carried out batch wise with respect to the liquid- and continuous to the gas phase. Gas was fed above the liquid surface at a small gas flow rate (almost 2.8 mL s^{-1} , *i.e.* 1.5 mm s^{-1}) for hindering any surface deformation and enabling a constant interfacial shear stress to be imposed.

The volumetric mass transfer coefficient ($k_L a$) was determined by applying the well-known dynamic method (nitrogen flushing, mass balance under unsteady-state condition). For that, an Unisense[®] microprobe (type OX 25-4046) was used. In the present case, the signal S of the polarographic probe (proportional to the equilibrium oxygen partial pressure in the bulk of the measured liquid) can be directly used for calculating $k_L a$, instead of the dissolved oxygen concentration which requires the knowledge of the oxygen solubility. Indeed, the volumetric mass transfer coefficient ($k_L a$) in the liquid medium is deduced from the slope of the curve described by:

$$\ln \frac{S^* - S}{S^* - S_0} = -k_L a \cdot t \quad (2)$$

which is equivalent to the following if the oxygen solubility is known:

$$\ln \frac{\alpha \cdot (S^* - S)}{\alpha \cdot (S^* - S_0)} = \ln \frac{C^* - C}{C^* - C_0} = -k_L a \cdot t \quad (3)$$

The duration of one experiment (*i.e.* one $k_L a$ measurement) was above 60 min, and was thus negligible when compared to the response time of the probe (0.5 s). Thanks to the hydrodynamics conditions imposed (low rotation speed and gas flow rate), the

Table 1

Properties of clean water and of the synthetic liquid media at 20 °C: surface tension ($\sigma_L \pm 0.5$ mNm), viscosity ($\mu_L \pm 10^{-3}$ mPa s), density ($\rho_L \pm 0.2$ kg m⁻³) and dissolved oxygen concentration at saturation ($C_L^* \pm 0.1$ g L⁻¹).

	C (g L ⁻¹) ^a	σ_L (mNm ⁻¹)	μ_L (mPa s)	ρ_L (kg m ⁻³)	C_L^* ($\times 10^{-3}$ g L ⁻¹)
Clean water	0	72.8	1.003	996.8	9.09
	1.6 (0.0138)	73.1	1.002	997.3	9.01
	2.4 (0.0207)	73.2		997.9	8.96
Salt (NaCl)	3.2 (0.0276)	73.4		998.7	8.92
	4 (0.0345)	73.6		999.2	8.88
	6 (0.0517)	73.8		1000.7	8.77
	32 (0.2750)	75.0		1018.9	7.52
	100 (0.8621)	76.1		1064.8	5.13
Sugar (glucose)	0.05	72.1	1.016	996.1	9.09
	5	71.4	1.112	996.3	9.07
	10	71.0	1.144	1000.2	9.04
	20	70.5	1.176	1003.9	9.00
	50	68.3	1.216	1015.4	8.86
Anionic surfactant [12]	100	64.3	1.263	1034.5	8.64
	0.05	69.8	1.003	996.2	9.09
	0.2	60.5	1.003	995.9	9.09
	1.9	40.7	1.003	996.1	9.09
	10	39.7	1.003	1000.0	9.09
Pure	33.0		35	1050.0	9.09

^a The ionic strength is put into brackets (mol L⁻¹).

interfacial area offered to mass transfer (a) could be reasonably defined by the ratio of the liquid surface (horizontal section area of the vessel) to the liquid volume ($a = 28.57$ m⁻¹). Liquid-side mass transfer coefficients were then calculated as:

$$k_L = \frac{k_L \cdot a}{a} \quad (4)$$

As reported in [12], the hydrodynamics conditions occurring in the present device (*i.e.* a gas small flow moving at a constant velocity above a slightly agitated liquid phase) provide that the gas–liquid mass transfer is mainly controlled by the level of turbulence imposed by the gas flow shearing the interface. In such conditions, the liquid-side mass transfer coefficient (k_L) depends on: (i) the interfacial momentum transfer velocity, U_i^* , which remains constant for similar phase properties, and on (ii) the Schmidt number, Sc . Consequently, the following expression was found by Hébrard

et al. [12]:

$$\frac{k_L}{U_i^*} \cdot Sc^{0.5} = C_1 \quad (5)$$

This is the general form of correlations or models related to absorption coefficients. The exponent of the Schmidt number depends on the nature of interfaces: it is equal to 1/2 for free surface [18] or completely mobile surface of bubbles [19,20], and to 2/3 for rigid/contaminated bubbles [21]. Considering $C_2 = C_1 \cdot U_i^*$, this induces:

$$D = \frac{\mu_L}{\rho_L} \cdot \left(\frac{k_L}{C_1 \cdot U_i^*} \right)^2 = \frac{\mu_L}{\rho_L} \cdot \left(\frac{k_L}{C_2} \right)^2 \quad (6)$$

The latter constant was experimentally determined in clean water at 20 °C, and validated for various temperatures and rotations

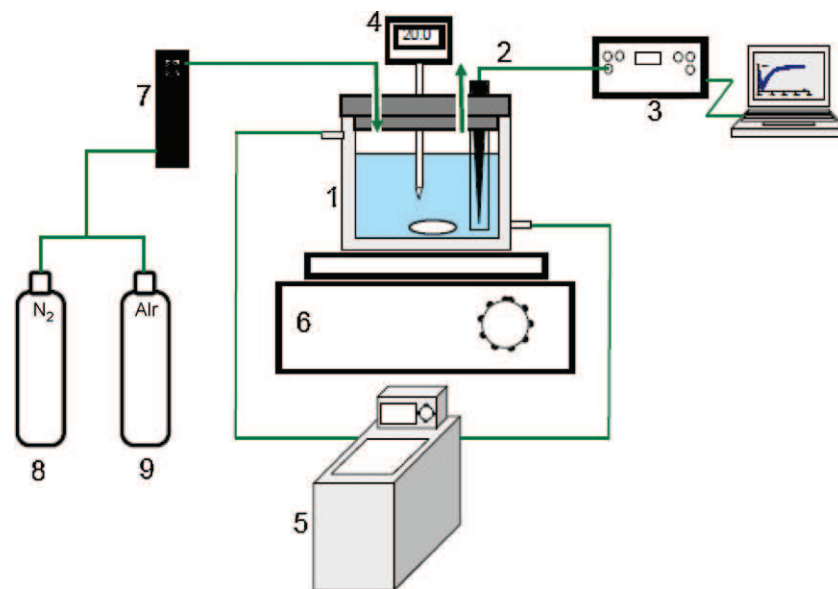


Fig. 1. Experimental set-up used for measuring oxygen diffusion coefficients: (1) double-wall vessel, (2) oxygen micro-probe Unisense®, (3) acquisition system, (4) thermometer, (5) thermo-regulation, (6) magnetic agitator, (7) gas flowmeter, (8) nitrogen supply, (9) air supply, (10) three-way valve.

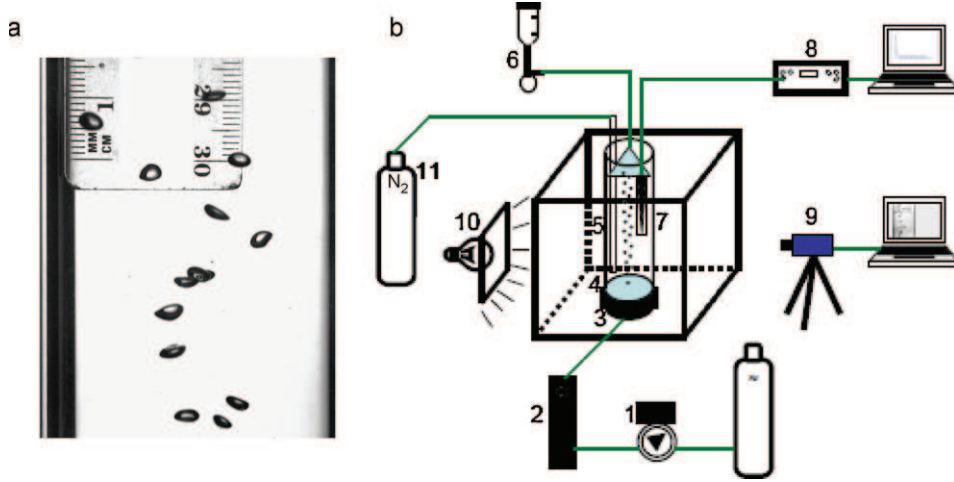


Fig. 2. (a) Illustration of a train of bubbles generated. (b) Experimental set-up used for measuring the liquid-side mass transfer coefficients associated with the latter train of bubbles: (1) pressure gauge, (2) gas flow meter, (3) electronic manometer, (4) square-sectional tank, (5) membrane sparger, (6) bubble column, (7) soap film meter, (8) chemical solution vessel, (9) oxygen microsensor, (10) acquisition system (camera, computer), (11) nitrogen pressure gauge, (12) agitation system.

speeds [12], leading to:

$$C_2 = 2.22 \cdot 10^{-4} \pm 0.21 \cdot 10^{-4} \text{ m s}^{-1} \quad (7)$$

This value of C_2 was assumed to be conserved for the synthetic liquid media under test. Note that this was verified as, the density of all liquid media under test did not differ from the one of water (Table 1), implying thus no changes in the interfacial momentum transfer velocity U_i^* [12]:

$$U_i^* = \sqrt{\frac{1/2 \cdot \rho_G \cdot f_i \cdot (U_G - U_L)^2}{\rho_L}} \quad (8)$$

Lastly, knowing the liquid mass transfer coefficient k_L ($k_L a$ measurements and Eq. (4)) and the liquid phase properties (Table 1), the diffusion coefficient of oxygen (D) could be easily deduced from Eqs. (6) and (7). The associated experimental uncertainty was estimated to 15%.

All the experiments were run between three and six times.

2.3. Experimental set-up for measuring the liquid-side mass transfer coefficients associated with a chain of bubbles (bubble column device)

The same device than Painmanakul et al. [9] was here used to generate a train of calibrated monodisperse bubbles (Fig. 2a). Experiments were carried out in a glass bubble column (0.043 m in diameter, 0.40 m in height, height of liquid $H_L = 0.23$ m), submerged in a water bath regulated in temperature (Fig. 2b). For all runs, the air sparger was an elastic membrane punctured with a single orifice and the gas flow rate was equal to 1.2 mL s^{-1} with sugar and salt and to 1.5 mL s^{-1} with surfactant. Nitrogen was flushed to fully remove dissolved oxygen in the synthetic liquid media, and also to maintain the oxygen concentration of the gas phase above the free surface null.

The volumetric mass transfer coefficients ($k_L a$) associated with the train of formed bubbles was measured using the sulphite static method [9]. For a given aeration time, the sodium sulphite (Na_2SO_3) was reacted with the oxygen transferred into the liquid phase by the generated bubbles. The remaining sulphite was determined by the iodometric method (oxidation of sulphites by iodine, and titration of excess iodine by sodium thiosulphate). As the initial oxygen concentration was kept at zero (nitrogen flushing), $k_L a$ can

be calculated from the following mass balance:

$$k_L a = \frac{(1/2)(M_{\text{O}_2}/M_{\text{Na}_2\text{SO}_3}) \cdot m_S}{t_{\text{aeration}} \cdot V_L \cdot C_L^*} \quad (9)$$

where M_{O_2} represents the molar mass of oxygen, $M_{\text{Na}_2\text{SO}_3}$ the molar mass of sodium sulphite, m_S the mass of Na_2SO_3 reacting with oxygen during the aeration phase (t_{aeration}), V_L the liquid volume of the glass column.

The dissolved oxygen concentration at saturation, C_L^* , was either measured or calculated for each liquid media. For water and salt solutions, C_L^* was directly measured using the polarographic probe UNISENSE, by first adjusting the correction factor proposed by UNISENSE® (e.g. the one linking the electrical signal given by the probe S to the oxygen concentration present in the liquid) as a function of the concentration in salts. For glucose solutions, C_L^* was firstly measured using an *in situ* chemical titration (i.e. the Winkler test [22,23]). As this method was difficult to implement with accuracy (in particular with respect to the artefact induced by atmospheric oxygen), the data reported by Slininger et al. [24] were used, they showed that a decrease of 5% in oxygen solubility took place when the glucose concentrations varied from 0 to 100 g L^{-1} . For surfactant solutions, it was assumed that C_L^* remained equal to those of clean water, considering the low concentration of surfactants present in water. All the values of C_L^* are reported in Table 1.

In this sulphite static method, the aeration time (2 min) and the initial sulphite mass (almost 60 mg) were optimised for ensuring a quantity of remaining sulphites sufficient for accurate titration while minimising the initial sulphite introduced. It was verified that the presence of sulphites changed neither the liquid properties nor the bubble characteristics.

During the aeration period, the interfacial area (a) was deduced from image acquisition and analysis [9,10], according to:

$$a = N_B \times \frac{S_B}{V_{\text{Total}}} = \left(f_B \cdot \frac{H_L}{U_B} \right) \times \frac{S_B}{A \cdot H_L + (f_B(H_L/U_B)) \cdot V_B} \quad (10)$$

where N_B represents the number of bubbles, U_B the terminal rising bubble velocity, A and H_L the cross-sectional area and the height of the glass column respectively. The image post-treatment assumed that the bubbles had an ellipsoidal shape (length l , height h , eccentricity $e = h/l$), the bubble diameter (d_B), volume (V_B) and surface area (S_B) were thus deduced from:

$$d_B = (l^2 \cdot h)^{1/3} \quad (11)$$

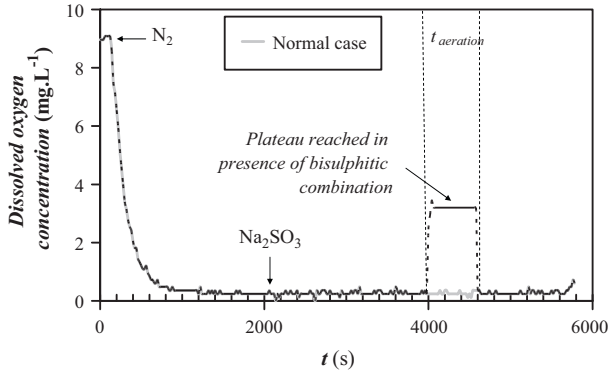


Fig. 3. Time-variation of dissolved oxygen concentration during the implementation of the sulphite static method for measuring $k_L a$.

$$V_B = \frac{\pi \cdot d_B^3}{6} \quad (12)$$

$$S_B = 2\pi \cdot \left[\frac{l^2}{4} + \left(\frac{l^2}{4} \times \frac{1}{2 \cdot e} \ln \left(\frac{1+e}{1-e} \right) \right) \right] \quad (13)$$

The bubble frequency (f_B) was calculated using two methods: (i) the ratio of air flow rate (soap flowmeter) to bubble volume and (ii) the direct counting of bubbles on the image sequence (time step of 2.5 ms). A good agreement between both methods was observed.

At last, the ratio of the coefficient $k_L a$ (sulphite static method) by the interfacial area a (image analysis) provided the liquid-side mass transfer coefficient k_L . The error induced by this method was approximately 20%, the iodometric titration being responsible of the main part of this experimental uncertainty.

It is important to note that the sulphite static method was successfully applied for all the media tested, except for the most concentrated solutions of glucose ($20 \leq C \leq 100 \text{ g L}^{-1}$). Under these conditions, the dissolved oxygen concentration did not remain at zero after air injection, but increased and reached a plateau corresponding to several mg L^{-1} , whatever the aeration time (this is illustrated in Fig. 3). This phenomenon was due to a bisulphite combination of the glucose molecules, as reported in the literature for high concentrations of glucose [25]. This “reaction” was reversible insofar as, if no air was introduced, the quantity of the sulphite ions remaining in solution after a given period of time were found (by titration) equal to the quantity initially introduced. When this bisulphitic combination occurred, the sulphite ions, initially introduced in slight excess, were no more available for consuming all the oxygen transferred, involving thus an increase of the oxygen dissolved concentration. The sulphite static method gave then erroneous values of $k_L a$, the dissolved oxygen concentration being no more equal to zero as stated in Eq. (9). Consequently, for the highest concentrations of glucose, it was chosen to implement the dynamic method (using the Unisense® microprobe) instead of the sulphite method, even if all the conditions required were not fully verified in the present bubble column device, in particular the perfectly mixed behaviour of the liquid phase.

3. Results and discussion

3.1. Influence of the substances contained in clean water on oxygen diffusion coefficients (D)

The oxygen diffusion coefficients obtained in synthetic liquid media are reported in Table 2. Firstly, the oxygen diffusion coefficient measured in clean water (at 20°C , $D_{\text{water}} = 1.98 \times 10^{-9} \text{ m}^2 \text{ s}^{-1}$) is in agreement with the mean value of $2 \times 10^{-9} \text{ m}^2 \text{ s}^{-1}$ encountered in literature [13,14,26,27].

Table 2

Oxygen diffusion coefficient in clean water and in synthetic liquid media (at 20°C , $\Delta D/D \approx 15\%$).

	$C \text{ (g L}^{-1}\text{)}$	$C \text{ (mol L}^{-1}\text{)}$	$D \text{ (}\times 10^{-9} \text{ m}^2 \text{ s}^{-1}\text{)}$
Clean water	0		1.98
Salt (NaCl)	1.6	2.76×10^{-2}	1.99
	2.4	4.14×10^{-2}	1.81
	3.2	5.52×10^{-2}	1.43
	4	6.90×10^{-2}	1.53
	6	1.03×10^{-1}	1.44
	32	5.52×10^{-1}	1.46
	100	1.72	1.16
Sugar (glucose)	0.05	2.8×10^{-4}	2.12
	5	2.78×10^{-2}	2.13
	10	5.56×10^{-2}	1.97
	20	1.11×10^{-1}	1.74
	50	2.78×10^{-1}	1.67
	100	5.56×10^{-1}	1.39
	Anionic surfactant [12]	0.05	1.3×10^{-4}
0.2		5.3×10^{-4}	1.38
1.9		5.00×10^{-3}	0.76
10		2.63×10^{-2}	0.70
Pure solution			

Fig. 4 compares, for various salt (NaCl) concentrations, the oxygen diffusion coefficients obtained in the present study and the following ones reported in the literature:

- Hung and Dinius [28] measured diffusivities of oxygen dissolved in aqueous solutions of various sodium-based salts by means of a diaphragm cell technique,
- Holtzapfle and Eubank [29] compared three models of diffusion of oxygen through aqueous salt solutions, based either on mole fraction, chemical potential or oxygen activity as the driving force. They demonstrated that the three models did not differ signif-

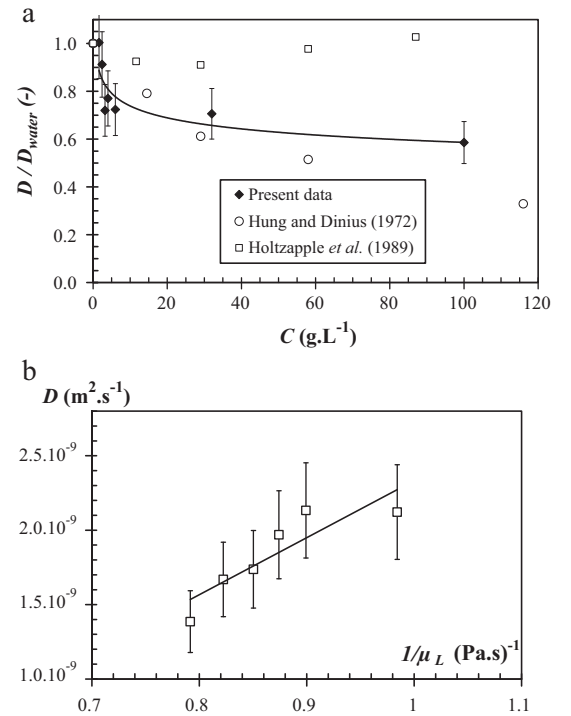


Fig. 4. (a) Comparison between the oxygen diffusion coefficients in aqueous solutions of salt measured and the ones reported in the literature. (b) Oxygen diffusion coefficient versus inverse of viscosity for aqueous solutions of glucose.

Table 3

Empirical coefficients relating to Eq. (15) for describing the variation of D/D_{water} with concentration.

	$(D/D_{\text{water}}) = 1 - k_{(17)} \cdot C^{n_{(17)}} \text{ (Eq. (17))}$		
	$k_{(17)}$	$n_{(17)}$	std (%)
Salt (NaCl)	0.179	0.180	6.5
Sugar (glucose)	0.0046	0.907	3.4
Surfactant	0.584	0.047	13.6

icantly in their predictions, except for extremely high oxygen partial pressures.

As shown in Fig. 4, our data are underestimated and overestimated when compared to the ones of [29] and [28] respectively. This discrepancy is not surprising as, at present, no generally accepted relationships for predicting the diffusivities of gases dissolved in electrolyte solutions exists, leading to various attempts of correlations, such as:

$$D = D_{\text{water}} \cdot (1 - k \cdot \sqrt{C}) \quad (14)$$

$$D = D_{\text{water}}(1 - A \cdot C) \quad (15)$$

$$\frac{D}{D_{\text{water}}} - 1 = \frac{B}{1+r} \cdot C \quad (16)$$

where k is an empirical constant [28], A an empirical constant [30], B the Jones and Dole viscosity coefficient and r a ratio involving the activation energies [31]. In the present study, these latter correlations do not give satisfactory results when fitting experimental data (least-square technique). The application of Eq. (14) to the present data leads to a constant k equal to 0.058 and 0.44 (std of 36%) when mass and molar concentrations are used respectively. This latter value is in good agreement with the one of 0.452 reported by [28]. However, we observe that the present relative change of D/D_{water} in salt solutions is better described (std of 6.5%) by:

$$D = D_{\text{water}} \cdot (1 - k_{(17)} \cdot C^{n_{(17)}}) \quad (17)$$

where $k_{(17)}$ and $n_{(17)}$ are empirical coefficients reported in Table 3 with C expressed in g L^{-1} .

Table 2 and Fig. 5 compare the variations of oxygen diffusion coefficients with concentrations for each type of synthetic media. As shown in Fig. 4 for salt, the oxygen diffusion coefficients in aqueous solutions of glucose and surfactant are noticeably smallest than in clean water, the lowest ones being obtained with surfactants. It is interesting to observe that, depending on the nature of the active substance, the rate of change of D/D_{water} with concentrations differs.

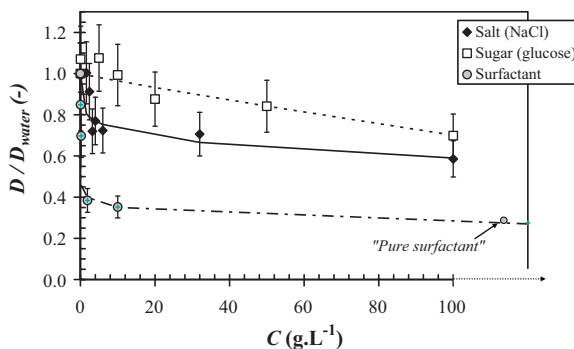


Fig. 5. Ratio between oxygen diffusion coefficients in synthetic liquid media and in clean water versus the concentration of the compound introduced (salt, sugar or surfactant) ($T = 20^\circ\text{C}$). The dotted and continuous line curves are issued from the modelling using Eq. (15) and the coefficients reported in Table 3.

For sugar solutions, the reduction of oxygen diffusion coefficients reaches 30% for the highest concentrations (100 g L^{-1}), leading to a minimal value of $1.39 \times 10^{-9} \text{ m}^2 \text{ s}^{-1}$. This latter value is fully relevant when compared to the results of Van Stroe-Biezen et al. [32] who measured, using an electrochemical method, the diffusion coefficient of oxygen in glucose solutions; indeed, these authors found a reduction in diffusivity of 26% when the glucose concentration varied from 0 to 100 g L^{-1} in their fermentation media. The decrease in viscosity with increasing concentrations of glucose (Table 1) is mainly responsible for such change in diffusion coefficients. This is illustrated in Fig. 4b where the usual dependence of D with the inverse of viscosity is verified, as predicted by the Stokes–Einstein equation and the correlation of Wilke and Chang (1954) [13]. The rate of change of D/D_{water} with concentrations in glucose is well correlated (std of 3.4%) by the same type of relationship than for salt (Eq. (17)): reported in Table 3, the empirical coefficients $k_{(17)}$ and $n_{(17)}$ are found smaller and higher than the ones calculated for salt and surfactant solutions respectively. Note that a further modelling would be also possible by drawing an analogy with the Sechenov equation commonly used to describe the effect of electrolytes on the solubility of gases in aqueous solutions [33], namely by:

$$\log\left(\frac{D}{D_{\text{water}}}\right) = -k_{(18)} \cdot C \quad (18)$$

where the constant $k_{(18)}$ would be thus analogous to the Sechenov constant involved when considering solubility in Eq. (18). The Sechenov constant depends on the nature of gas phase, temperature and species in solution, and then can be predicted by using ion-specific constants for salting-out and ionic strength of ions. Schumpe and Deckwer [34] extended this model of solubility when organic substances (like methanol, ethanol, propanol or glycerol) were present, and found Sechenov constants ranged between 0.1 and 0.4 (using C in mol L^{-1}). When Eq. (18) is applied for predicting the diffusion coefficients in glucose solutions, $k_{(18)}$ is found equal to 1.6×10^{-3} (using C in g L^{-1}) and to 0.28 (using C in mol L^{-1}) with a std of almost 12%. The latter value has the same order of magnitude than the Sechenov constants found by [34] for solubility. This comparison would suggest that, concerning the influence of sugar, a parallel between both solubility and diffusion coefficient of oxygen would be drawn: other types of organic substances should be tested to definitively confirm this behaviour. Note that the modelling using Eq. (18): (i) leads to higher standard deviations (approximate fitting) than the one using Eq. (17) and (ii) is surprisingly not adapted for the synthetic media containing NaCl (high std).

In presence of surfactants, the diffusion of oxygen does not involve exactly the same mechanisms that the ones occurring in aqueous solutions of salt or glucose, due to the dynamics of surfactant adsorption/desorption at the gas–liquid interface and to the associated partial or full surface contamination; the term of *apparent* or *effective* diffusivity would be thus rigorously more appropriated. Nevertheless, the comparison between the time scales of the different phenomena involved (see Section 2.1) suggests that, in the present experiments, the adsorption equilibrium of the surfactant molecules at the gas–liquid interface is reached. This would induce that the diffusion coefficients measured are time-independent. Fig. 5 shows that, in presence of surfactants, the decrease of oxygen diffusion coefficients with concentration is strongly pronounced: for concentrations above the critical micellar concentration (1.9 g L^{-1}), D becomes almost constant around $0.7 \times 10^{-9} \text{ m}^2 \text{ s}^{-1}$, namely about 0.4 times the value for clean water. Note that the oxygen diffusion coefficient in a pure solution of surfactant (Fig. 5) is equal to $0.55 \times 10^{-9} \text{ m}^2 \text{ s}^{-1}$ (data from [12]), and has thus the same order of magnitude than the ones measured for $C > \text{CMC}$. Such result implies that, even if it is not sure that

Table 4

Results dealing with experiments carried out on a train of bubbles in clean water and in synthetic liquid media (at 20 °C): bubble diameter, terminal rising bubble velocity, bubble Reynolds number, liquid-side mass transfer coefficient, Schmidt number and Sherwood number.

	C (g L ⁻¹)	d_B (mm)	f_B (Hz)	U_B (m s ⁻¹)	Re_B	k_L (10 ⁻⁴ m s ⁻¹)	Sc	Sh
Clean water	0	3.9	40.3	0.29	1118	4.6	507	894
Salt (NaCl)	1.6	4.2	34	0.29	1187	4.9	505	1028
	2.4	4.0	35.6	0.30	1183	5.5	555	1203
	3.2	3.9	41.7	0.27	1039	4.5	703	1227
	4	3.5	55.5	0.29	1001	4.1	657	933
	6	3.7	44.6	0.29	1080	4.7	698	1221
	32	3.6	50.9	0.30	1089	4.4	703	1126
	100	3.1	79.0	0.29	964	3.6	810	956
Sugar (Glucose)	0.05	4.1	39.0	0.29	1146	4.6	481	887
	5	3.9	40.3	0.29	1003	3.8	523	682
	10	3.8	43.6	0.29	958	3.5	581	673
	20	3.4	59.9	0.29	817	2.6	674	501
	50	3.3	66.6	0.30	806	2.5	718	481
	100	3.2	69.0	0.28	733	2.2	881	500
	Anionic surfactant	0.05	5.16	22.7	0.22	1102	2.9	598
0.2		5.29	20.3	0.22	1129	2.1	728	792
1.9		5.17	22	0.22	1130	1.7	1322	1120

the bulk solution is really homogeneous when $C < \text{CMC}$, the notion of (apparent/effective) diffusion is transposable within a thickness around the gas–liquid interface defined by one or several surfactant mono-layers. The variation of D with surfactant concentration can be satisfactorily modelled either using Eq. (17) (see Table 3) or according to a power law:

$$\frac{D}{D_{\text{water}}} = k_{(19)} \cdot C^{n_{(19)}} \quad (19)$$

with $k_{(19)} = 0.512$ and $n_{(19)} = -0.15$ (std of 6%).

It is interesting to face all the previous results with the work of Ho and Ju [35] who highlighted a similar behaviour when measured effective oxygen diffusion coefficients in various fermentation media (*Saccharomyces cerevisiae*, *Escherichia coli* and *Penicillium chrysogenum*). Whatever the culture media, a linear decrease of D for increasing cell volume fractions was systematically observed, mainly explained by the spatial hindering effect of cells on the motion of diffusing oxygen molecules. To get some orders of magnitude, some results obtained by [35] are here reminded: for *S. cerevisiae* at 116 g dry cells/L $D = 1.57 \times 10^{-9} \text{ m}^2 \text{ s}^{-1}$, for *E. coli* at 55 g dry cells/L $D = 1.76 \times 10^{-9} \text{ m}^2 \text{ s}^{-1}$ and for *P. chrysogenum* at 37 g dry cells/L $D = 1.03 \times 10^{-9} \text{ m}^2 \text{ s}^{-1}$. In the present work, the mechanisms controlling the reduction of oxygen diffusion coefficients are certainly different, as rather linked to ionic strength, steric, viscosity and/or molecule adsorption effects, but their consequences on D are comparable.

To conclude, all these findings illustrate that the kind of the active substances has a major effect, at a given concentration, on the value of oxygen diffusion coefficients, but also on its rate of change with respect to clean water. To quantify these tendencies, attempts of modelling have been performed using various (semi)-empirical correlations issued from literature; in particular, the use of Eq. (17) has enabled to highlight the strongest impact of surfactant on D/D_{water} when compared to glucose or salt ($n_{(17)\text{surfactant}} < n_{(17)\text{salt}} < n_{(17)\text{glucose}}$, Table 3).

3.2. Influence of the substances contained in water on liquid-side mass transfer coefficients (k_L)

3.2.1. Characteristics of the bubbles generated

The experiments on a train of bubbles rising in a quiescent liquid phase were run in the same synthetic liquid media than the ones used for measuring oxygen diffusion coefficients. In Table 4, the measured bubble diameter, frequency, terminal rising velocity and Reynolds number are firstly reported for each liquid media.

For aqueous solutions of salt and sugar, the image analysis has revealed that the bubble diameters remain equal to the ones measured in clean water ($d_B = 3.9 \pm 0.3 \text{ mm}$), apart from the highest concentrations (e.g. $C = 100 \text{ g L}^{-1}$ for salt and $C > 20 \text{ g L}^{-1}$ for glucose) where a change appears ($3.1 < d_B < 3.4 \text{ mm}$) due to the changes in surface tension and/or viscosity (see Table 1). Almost the same tendency is observed for bubble frequencies (f_B) and terminal rising velocities (U_B). Note that the surface tensions of salt media slightly higher than in water (Table 1) have no major effect on bubble diameter, but induce a rise of bubble frequencies (from 40 to 79 s⁻¹). At last, the synthetic liquid media containing salts do not modify significantly the bubble Reynolds number ($Re_B = 1103 \pm 86$) when compared to clean water, even if, for the most concentrated solution, Re_B falls down to 964. On the contrary, the bubble Reynolds numbers associated with aqueous solutions of glucose decrease progressively with concentrations (from 1146 to 733), as a direct consequence of the rise in viscosity (Table 1).

The data dealing with surfactants reported in Table 4 have been extracted from [10]. They show that, whatever the concentrations, the contamination by anionic surfactants induces bubbles of constant diameters ($d_B = 5.2 \pm 0.1 \text{ mm}$) and constant frequencies ($f_B = 21.6 \pm 1.2 \text{ s}^{-1}$). Note that, if these bubble sizes are greater than those obtained in clean water and in aqueous solutions of salt and glucose, it is only because an higher gas flow rate was operated ($Q_G = 1.5 \text{ mL s}^{-1}$) instead of 1.2 mL s^{-1} (data reported from [10]). Nevertheless, the bubble Reynolds numbers in presence of surfactants have finally the same order of magnitude than in others cases ($Re_B = 1120 \pm 16$).

3.2.2. Liquid-side mass transfer coefficients

Table 4 reports, for each aqueous solution of salt, sugar or surfactant, the liquid-side mass transfer coefficients k_L measured for the train of rising bubbles. It clearly illustrates that, whatever its nature, the presence of the active substance in water noticeably affects the mass transfer coefficient when compared to clean water, and that, at a given molar concentration, the strongest and smallest impacts on k_L are induced by the presence of surfactants and salt respectively. Fig. 6, in which the ratio between liquid-side mass transfer coefficients in synthetic liquid media and in clean water ($k_L/k_{L\text{water}}$) as a function of the concentrations in salt, sugar or surfactant are reported, confirms the latter tendencies.

For glucose, a major reduction in k_L is induced: 18% at $C = 5 \text{ g L}^{-1}$, 24% at $C = 10 \text{ g L}^{-1}$ and 53% at $C = 100 \text{ g L}^{-1}$. This variation can be successfully described by the same type of relationships than the

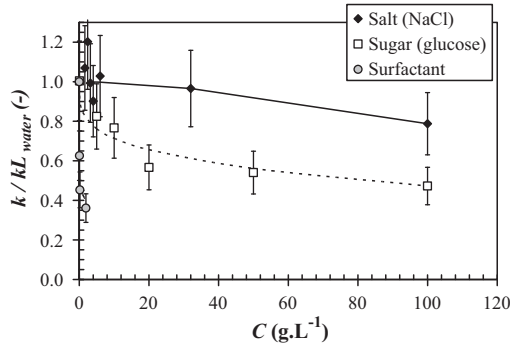


Fig. 6. Ratio between liquid-side mass transfer coefficients in synthetic liquid media and in clean water versus the concentration of the compound introduced (salt, sugar or surfactant) ($T=20^\circ\text{C}$).

ones used for diffusion coefficients (Eqs. (15) and (17)), namely:

$$\frac{k_L}{k_{L,\text{water}}} = 1 - k_{(20)} \cdot C^{n_{(20)}} \quad (20)$$

or,

$$\frac{k_L}{k_{L,\text{water}}} = k_{(21)} C^{n_{(21)}} \quad (21)$$

where $k_{(20)}$, $n_{(20)}$, $k_{(21)}$ and $n_{(21)}$, are empirical coefficients reported in Table 5. Note that for aqueous solutions of glucose: (i) the coefficients $k_{(20)}$ and $n_{(20)}$ differ from the ones found for describing the rate of change of D/D_{water} (see Table 3), (ii) the fitting with respect to experimental data is better with Eq. (20) than with Eq. (21) (smaller std), (iii) the Sechenov-type relationship used for diffusion coefficients (Eq. (18)) is not at all adapted for mass transfer coefficients.

For salt solutions, the rate of change in mass transfer coefficients with respect to clean water is less pronounced than for glucose, but still exists: at 100 g L^{-1} , $k_L/k_{L,\text{water}}=0.79$ against 0.47 for glucose. It is interesting to observe that for $C \leq 2.4 \text{ g L}^{-1}$, higher k_L than in water can be distinguished (these results are reproducible); as this deviation from water is at the same order of magnitude than the experimental uncertainties (20%), some caution should be taken for analysis. Nevertheless, this kind of phenomenon, e.g. an increase of k_L , has been already observed, for example at low concentrations of short-chain surfactant molecules for carbon dioxide–water absorption process [36] or in presence of ethanol in a gas–liquid deshumidifier [37]. The latter enhancement of mass transfer is usually attributed by the workers to the induced Marangoni effect, namely to the generation of interfacial turbulence caused by surface tension gradients, and producing an increase in the renewal process of the liquid elements and thus a rise in the driving force corresponding to the absorption process. Deeper investigations will be required in the future to verify this assumption (*i.e.* the increase of mass transfer by Marangoni effect) in the case of salt solutions.

Like for glucose, the type of modelling used in Eq. (20) is well transposable (*i.e.* with a std of 3%) to describe the rate of change of $k_L/k_{L,\text{water}}$ for salt concentrations higher than 2.4 g L^{-1} . The coefficients $k_{(20)}$ and $n_{(20)}$ determined (Table 5) differ here also from the

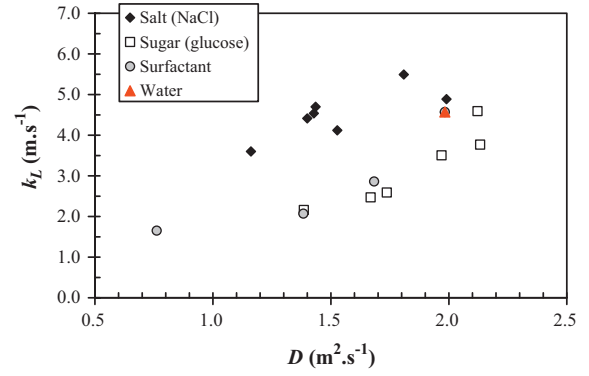


Fig. 7. Liquid-side mass transfer coefficients versus oxygen diffusion coefficients ($T=20^\circ\text{C}$).

ones found for describing the rate of change of D/D_{water} . Note that neither Eq. (21) nor the relationships like Eq. (14) are adapted for salt media (high std).

Concerning the surfactant solutions, the impact is more pronounced than for the other active substances: k_L is here diminished from 37% at $C=0.05 \text{ g L}^{-1}$, from 55% at $C=0.2 \text{ g L}^{-1}$ and from 64% at $C=1.9 \text{ g L}^{-1}$. Contrary to salt and glucose solutions, the rate of change of $k_L/k_{L,\text{water}}$ with surfactant concentration can be perfectly modelled (std of 11%) using Eq. (20) and the *same* coefficients $k_{(12)}$ and $n_{(12)}$ than for diffusion coefficients. An alternative is to use Eq. (21) (see Table 5).

Finally, from these findings, the key role played by the nature of the active substance on the resistance to mass transport in the liquid side is clearly confirmed. Moreover, for a given substance, it has been demonstrated that the relationships modelling the rates of change of $k_L/k_{L,\text{water}}$ and of D/D_{water} with concentration have remarkably the same form (Eq. (20)) with different empirical coefficients (except for surfactants). Therefore, it becomes essential to pay a particular attention on the establishment of the potential relationships between the ratios ($D_{\text{medium}}/D_{\text{water}}$) and ($k_{L,\text{medium}}/k_{L,\text{water}}$).

3.3. Relationship between liquid-side mass transfer coefficients and oxygen diffusion coefficients

In Fig. 7 are reported, for each synthetic liquid medium, the variations of liquid-side mass transfer coefficients k_L (obtained on a train of bubbles) with oxygen diffusion coefficients D . As reference, the case of clean water is plotted as a red triangle symbol: $k_{L,\text{water}}=4.6 \times 10^{-4} \text{ m s}^{-1}$ is in agreement with literature data [2]. Whatever the active substance, the simultaneous decrease of k_L with D is clearly highlighted, and these even when experimental uncertainties are integrated ($\pm 15\%$ for D and $\pm 20\%$ for k_L). It is important to note that, for all the aqueous solutions of salt (except for the highest concentrated), the properties of clean water (ρ_L , μ_L , σ_L) are conserved as well as the global hydrodynamics conditions controlling the bubbles generated (Re_B). The decrease in the resistance to mass transport in the liquid side (k_L) can be thus attributed to the change in oxygen diffusion coefficients, namely

Table 5
Empirical coefficients relating to Eqs. (18) and (19) for describing the variation of $k_L/k_{L,\text{water}}$ with concentration.

	$(k_L/k_{L,\text{water}}) = 1 - k_{(20)} C^{n_{(20)}} \text{ (Eq. (20))}$			$(k_L/k_{L,\text{water}}) = k_{(21)} C^{n_{(21)}} \text{ (Eq. (21))}$		
	$k_{(20)}$	$n_{(20)}$	std (%)	$k_{(21)}$	$n_{(21)}$	std (%)
Salt (NaCl)	1.34×10^{-4}	1.599	2.9	–	–	–
Sugar (glucose)	0.155	0.266	5.1	0.826	–0.098	16
Surfactant	0.584	0.047	11	0.386	–0.15	5

to the rise of the Schmidt number Sc (Table 3). With the solutions containing glucose, the case is the same, but coupled with the effect of viscosity. Even if change, the change in viscosity should induce some modifications in the local hydrodynamics in the vicinity of the interface, the liquid side mass transfer coefficient k_L is also affected by a modification of diffusion coefficient.

The contamination of clean water by surfactant induces some changes in surface tension (progressive coverage of bubble surface by surfactant molecules) when compared with water. However, the bubble Reynolds numbers remaining almost constant for all concentrations, this is, in this case also, the change of oxygen diffusion coefficients which is responsible for the reduction in liquid-side mass transfer coefficients.

At this stage, the establishment of a fine model describing the variation of k_L with D is premature, as: (i) the experimental uncertainties on both parameters are not sufficiently small and (ii) the number and the type of active substance to introduce in clean water should be extended to cover a more representative domain. Nevertheless, the latter results point out an important issue, namely that the rate of change of k_L with D is strongly correlated with the nature of the compound present in water. In the future, the ability to complete the database related to oxygen diffusion coefficients in complex media will thus constitute a key step for understanding and modelling properly the gas-liquid mass transfer phenomena.

4. Conclusions

Specific experiments were run to study the influence on the liquid phase composition on oxygen diffusion coefficients D . A focus was made on the addition in clean water of three types of substances commonly encountered in biological media: a salt (NaCl), a sugar (glucose) and an anionic surfactant. The experimental device and methodology developed by Hébrard et al. [12] were used for measuring D . For all cases, oxygen diffusion coefficients were lowered when compared to clean water, and, depending on the nature of the substance added, this rate of change of D with concentration differ. To quantify these tendencies, attempts of modelling were performed using various (semi)-empirical correlations issued from literature; in particular, the use of Eq. (17) enabled to highlight the strongest impact of surfactant on D/D_{water} when compared to glucose or salt.

In a second time, experiments on a train of bubbles rising in a quiescent liquid phase were carried out in the same synthetic liquid media, aiming at determining liquid-side mass transfer coefficients (Painmanakul et al. [9]). The image analysis technique showed firstly that the hydrodynamic conditions controlling the bubbles generated (*i.e.* bubble Reynolds number) occurring in clean water were almost conserved, except for the most concentrated solution of salt and glucose. Afterwards, the key role played by the nature of the active substance on the resistance to mass transport in the liquid side was clearly confirmed. For a given substance, it was demonstrated that the relationships modelling the rates of change of $k_L/k_{L,\text{water}}$ and of D/D_{water} with concentration had remarkably the same form (Eq. (20)) with different empirical coefficients (except for surfactants).

The present study clearly highlighted the need to complete the database related to oxygen diffusion coefficients in complex media, this condition being imperatively required to describe and to model properly the gas-liquid mass transfer phenomena.

References

[1] F. Garcia-Ochoa, E. Gomez, Bioreactor scale-up and oxygen transfer rate in microbial processes: an overview, *Biotechnology Advances* 27 (2) (2009) 153–176.

[2] M. Roustan, *Transferts gaz-liquide dans les procédés de traitement des eaux et des effluents gazeux*, Editions Dec & Doc, Paris, 2003.

[3] M. Zlokarnik, Sorption characteristics of slot injectors and their dependency on the coalescence behaviour of the system, *Chemical Engineering Science* 34 (1979) 1265–1271.

[4] M. Fyferling, J.-L. Uribelarrea, G. Goma, C. Molina-Jouve, Oxygen transfer in intensive microbial culture, *Bioprocess and Biosystems Engineering* 31 (6) (2008) 595–604.

[5] A. Sundararajan, L.-K. Ju, Biological oxygen transfer enhancement in bioreactors, *TranslChemE* 71 C (1993) 221–223.

[6] B. Cuenot, J. Magnaudet, B. Spennato, The effects of slightly soluble surfactants on the flow around a spherical bubble, *Journal of Fluid Mechanics* 399 (1997) 25–53.

[7] S.S. Alves, S.P. Orvalho, J.M.T. Vasconcelos, Effect of bubble contamination on rise velocity and mass transfer, *Chemical Engineering Science* 60 (2005) 1–9.

[8] A. Dani, A. Cockx, P. Guiraud, Direct numerical simulation of mass transfer from spherical bubbles: the effect of interface contamination at low Reynolds numbers, *International Journal of Chemical Reactor Engineering* 4 (2006) A2.

[9] P. Painmanakul, K. Loubière, G. Hébrard, M. Mietton-Peuchot, M. Roustan, Effect of surfactants on liquid-side mass transfer coefficients, *Chemical Engineering Science* 60 (2005) 6480–6491.

[10] R. Sardeing, P. Painmanakul, G. Hébrard, Effect of surfactants on liquid-side mass transfer coefficients in gas-liquid systems: a first step to modelling, *Chemical Engineering Science* 61 (2006) 6249–6260.

[11] D. Rosso, D.L. Huo, M.K. Stenstrom, Effects of interfacial surfactant contamination on bubble gas transfer, *Chemical Engineering Science* 61 (2006) 5500–5514.

[12] G. Hébrard, J. Zeng, K. Loubière, Effects of surfactants on liquid side mass transfer coefficients: a new insight, *Chemical Engineering Journal* 148 (1) (2009) 132–138.

[13] C.R. Wilke, P. Chang, Correlation of diffusion coefficients in dilute solutions, *AIChE Journal* 1 (2) (1955) 264–270.

[14] E.G. Scheibel, *Physical chemistry in chemical engineering design*, Industrial and Engineering Chemistry Fundamentals (1954) 46.

[15] M. Martin, F.J. Montes, M.A. Galan, Theoretical modelling of the effect of surface active species on the mass transfer rates in bubble column reactors, *Chemical Engineering Journal* (2009) (available on line doi:10.1016/j.ccej.2009.08.009).

[16] K. Loubière, G. Hébrard, Influence of liquid surface tension (surfactants) on bubble formation at rigid and flexible orifices, *Chemical Engineering and Processing* 43 (2004) 1361–1369.

[17] M.C. Ruzicka, M.M. Vecer, S. Orvalho, J. Drahos, Effect of surfactant on homogeneous regime stability in bubble column, *Chemical Engineering Science* 63 (2008) 951–967.

[18] I. Calmet, J. Magnaudet, Transfert de masse à l'interface d'un film turbulent libre ou cisailé, *Revue Generale Thermique* 37 (1988) 769–780.

[19] P.H. Calderbank, M.B. Moo-Young, The continuous phase heat and mass transfer properties of dispersions, *Chemical Engineering Science* 16 (1961) 39–61.

[20] R. Higbie, The rate of absorption of a pure gas into a still liquid during short periods of exposure, *Transactions of The American Institution Chemical Engineers* 35 (1935) 36–60.

[21] N. Frössling, Über die Verdunstung fallenden Tropfen, *Gerlans Beitäge Geophysik* 52 (1938) 170–216.

[22] L. Winkler, Die Bestimmung des in Wasser Gelösten Sauerstoffes, *Berichte der Deutschen Chemischen Gesellschaft* 21 (1888) 2843–2855.

[23] Norme NF EN 25813 (ISO 5813), Dosage de l'oxygène dissous: méthode iodométrique, AFNOR, 1993.

[24] P.J. Slininger, R.J. Petroski, R.J. Bothast, M.R. Ladisch, M.R. Okos, Measurement of oxygen solubility in fermentation media—A colorimetric method, *Biotechnology and Bioengineering* 33 (5) (1989) 578–583.

[25] B.W. Zocklein, K.C. Fugelsang, B.H. Gump, F.S. Nury, *Wine Analysis and Production*, Chapman and Hall, New York, 1995 (Originally published).

[26] R.H. Perry, D.W. Green, *Perry's Chemical Engineer's Handbook*, 7th ed., McGraw-Hill, New York, 1997.

[27] C.O. Bennett, J.E. Myers, I.J.E., *Momentum, Heat and Mass Transfer*, 2nd ed., McGraw-Hill Chemical Engineering Series, 1967.

[28] G.W. Hung, R.H. Dinius, Diffusivity of oxygen in electrolyte solutions, *Journal of Chemical and Engineering Data* 17 (4) (1972) 449–451.

[29] M.T. Holtzapfel, P.T. Eubank, A comparison of three models for the diffusion of oxygen in electrolyte solutions, *Biotechnology and Bioengineering* 34 (1989) 964–970.

[30] G.A. Ratcliff, J.C. Holdcroft, *Transactions of the Institution of Chemical Engineering (London)* 45 (1963) 315.

[31] R.J. Rodolfsky, *Journal of the American Chemical Society* 8 (1958) 4442.

[32] S.A.M. Van Stroe-Biezen, A.P.M. Janssen, L.J.J. Janssen, Solubility of oxygen solutions, *Analytica Chimica Acta* 280 (1993) 217–222.

[33] A. Schumpe, I. Adler, W.-D. Deckwer, Estimation of O₂ and CO₂ solubilities in electrolytes, *Biotechnology and Bioengineering* 20 (1978) 145–150.

[34] A. Schumpe, W.-D. Deckwer, Estimation of O₂ and CO₂ solubilities in fermentation media, *Biotechnology and Bioengineering* 21 (1979) 1075–1078.

- [35] C.S. Ho, L.-K. Ju, Effects of microorganisms on effective oxygen diffusion coefficients and solubilities in fermentation media, *Biotechnology and Bioengineering* 32 (1988) 313–325.
- [36] D. Gomez-Diaz, J.M. Navaza, B. Sanjurjo, Mass-transfer enhancement or reduction by surfactant presence at a gas-liquid interface, *Industrial and Engineering Chemical Research* 48 (2009) 2671–2677.
- [37] N.-H. Yang, Y.-J. Chen, C.-C. Liao, T.-W. Chung, Improved absorption in gas-liquid systems by the addition of a low surface tension component in the gas and/or liquid phase, *Industrial and Engineering Chemical Research* 47 (2008) 8823–8827.